

# From RDMA to RDCA: Toward High-Speed Last Mile of Data Center Networks Using Remote Direct Cache Access

Qiang Li<sup>◇</sup>, Qiao Xiang<sup>†</sup>, Derui Liu<sup>◇</sup>, Yuxin Wang<sup>†◇</sup>, Haonan Qiu<sup>◇</sup>, Xiaoliang Wang<sup>‡</sup>, Jie Zhang<sup>◇</sup>,  
Ridi Wen<sup>†◇</sup>, Haohao Song<sup>†◇</sup>, Gexiao Tian<sup>◇</sup>, Chenyang Huang<sup>†</sup>, Lulu Chen<sup>△◇</sup>, Shaozong Liu<sup>◇</sup>,  
Yaohui Wu<sup>◇</sup>, Zhiwu Wu<sup>◇</sup>, Zicheng Luo<sup>◇</sup>, Yuchao Shao<sup>◇</sup>, Chao Han<sup>◇</sup>, Zhongjie Wu<sup>◇</sup>,  
Jianbo Dong<sup>◇</sup>, Zheng Cao<sup>◇</sup>, Jinbo Wu<sup>◇</sup>, Jiwu Shu<sup>†</sup>, Jiasheng Wu<sup>◇</sup>,  
<sup>◇</sup>Alibaba Group, <sup>†</sup>Xiamen University, <sup>‡</sup>Nanjing University, <sup>◇</sup>Peking University, <sup>△</sup>Fudan University

## Abstract

We conduct a systematic measurement study on the receiver host datapath from the RDMA-capable NIC (RNIC) to applications in a production data center network (DCN). We find that the memory bandwidth is the bottleneck in this last mile of RDMA and leads to a significant drop in network throughput and a large increase in latency. In particular, the RNIC cannot acquire enough memory bandwidth due to the high contention between RNIC and CPU. Consequently, in-flight packets queue up in the RNIC buffer, resulting in overflowed packet loss and triggering the congestion control mechanism even if the network bandwidth is not fully utilized.

To tackle this problem, we propose to move the memory out of the receiver host datapath and reserve a small area in the last level cache (LLC) for the RNIC to send data to, enabling remote hosts to directly access the receiver cache (RDCA). Our key observation is that in typical DCN workloads, the time-span data spent in memory after leaving the RNIC is very short (*e.g.*, hundreds of  $\mu$ s on average). Therefore, it is possible to recycle a small cache area to support RNIC operations at line rate (*e.g.*, 200 Gbps). We design *Jet*, a cache-centric receiver service realizing RDCA with a cache-resident buffer pool, a swift cache recycle controller and a cache-pressure-aware escape controller. Experiments in testbed and production DCN show that *Jet* improves throughput by up to 2.11x and P99 latency by up to 86.4% and consumes only 12 MB LLC.

## 1 Introduction

Data center (DC) applications such as storage [1, 2], high-performance computing [3, 4], data analytics [5, 6], and machine learning [7, 8] have stringent performance requirements on high throughput and low tail latencies. Remote direct memory access (RDMA) is an appealing solution to meet these requirements because of its low-latency, CPU-bypassing primitives. Multiple major DC operators have deployed RDMA in their production DCNs [9–12]. They design different mechanisms (*e.g.*, congestion control [13, 14], scalable RPC [15, 16], and new features on programmable NIC [17–19]) to ensure RDMA operates efficiently in large-scale, IP-routed DCNs.

These mechanisms focus on smoothing RDMA operations in network fabrics (*e.g.*, switches and RNICs), because the conventional wisdom is that network is usually the bottleneck.

**Finding in a production DCN: the memory bandwidth bottleneck limits the performance of RDMA.** (§2.1) A systematic measurement study in a production DCN finds that the memory bandwidth bottleneck in the *receiver host datapath* from the RNIC to applications limits RDMA from delivering data at a high bandwidth and a low latency. To be concrete, when the RNIC performs DMA operations to send received messages to memory, it causes a high contention on memory bandwidth between RNIC and CPU performing computations (*e.g.*, in-memory data analytics, data replication, and garbage collection). Under this contention, the RNIC cannot acquire sufficient memory bandwidth to send received packets to memory. The RNIC buffer is filled with in-flight packets and eventually drops overflowed ones. It triggers the congestion control (Figure 1) even if the network is not fully utilized, leading to a large throughput drop (*e.g.*, ~15% drop per server in the production DCN) and a considerable increase in latency. Our recent conversations with other DC operators reveal that this phenomenon is not an isolated finding but a universal one. One operator recently published this issue [20].

This memory-bandwidth-induced RDMA performance degradation can be alleviated by optimizing the memory usage of applications and RNIC [15, 21–23]. However, these solutions are mostly tailored for specific applications and specific RDMA verbs. It is also unclear whether they can scale up with the bandwidth expansion of RDMA technologies (*e.g.*, 100 Gbps/port in 2016 [24] and 400 Gbps/port in 2021 [25]). Some recent studies propose redesigning RNIC by adding memory modules [26, 27]. However, they require upgrading DCN with specialized, non-commodity RNICs [28].

**Proposal: move memory out of the receiver host datapath and put in the reserved cache.** (§2.2) Instead of continuing to optimize RNIC and applications for more efficient use of memory bandwidth, we embrace a bold proposal: move memory out of the receiver host datapath and reserve a small area in the cache, which has a much higher bandwidth than

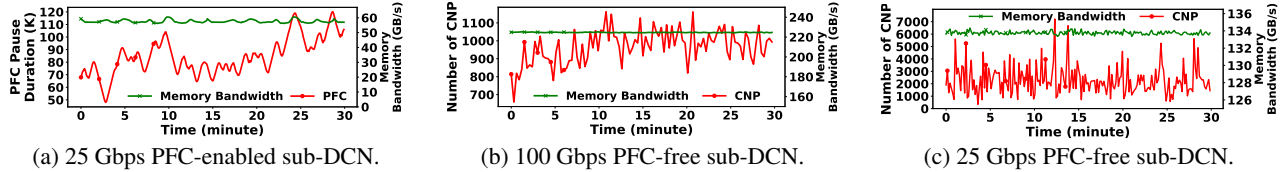


Figure 1: Memory bandwidth and PFC duration/CNP in throughput-drop incidents in a production DCN. memory, for the RNIC to forward the received messages to. In this way, senders do not access the receiver’s memory but its cache instead. We coin the name remote direct cache access (RDCA) for this design. RDCA allows the RNIC to enjoy the high bandwidth of cache. As a result, there will be no memory-bandwidth-induced packet loss, and the RNIC can operate at line rate (*e.g.*, 200 Gbps).

The key observation supporting the feasibility of RDCA is that in typical DCN workloads (*e.g.*, storage, machine learning, and HPC), the post-RNIC timespan (*i.e.*, the timespan data spent in memory after leaving RNIC) is very short (*i.e.*, hundreds of  $\mu$ s in average). As such, based on Little’s law [29], the average amount of data the RNIC stores in the memory is small enough to be held in the last-level cache (LLC) of commodity servers. For example, when the average of this post-RNIC timespan is 200  $\mu$ s, for a dual-port 100 Gbps RNIC, we only need 5 MB for temporally storing the data leaving RNIC on average while Intel Xeon E5 provides up to 20 MB LLC.

Direct Cache Access (DCA) [30] and Data Direct I/O (DDIO) [31] take the first steps in leveraging cache for fast packet processing. DCA prefetches I/O metadata to cache (*e.g.*, descriptors and packet header) but requires the RNIC to access data in memory [31, 32]. DDIO lets RNIC access data in the LLC and introduces write allocate and write update operations to update the cache. DDIO is deployed in Intel Xeon E5 CPU [31], but its benefit in high-speed networks is small. This issue, known as the leaky DMA problem [33–36], is due to the frequent write allocate triggered by new incoming messages, forcing the RNIC to access data in memory. In contrast, we go beyond the passive designs of DCA and DDIO and show that with a careful design, we can recycle a small area of LLC to support RNIC operations at line rate.

**Jet: a cache-centric service realizing RDCA (§2.2, §3, §4).** Although the idea makes sense on a high level, realizing RDCA has challenges. First, although the actual total space needed for temporally storing messages leaving RNIC is small, RDMA queue pairs (QPs) over-reserve buffers, resulting in inefficient space statistic multiplexing. Second, reserving a part of the LLC would cause a higher contention on the remaining LLC among other processes. As such, it is desirable to reduce data’s post-RNIC timespan so that RDCA consumes a smaller LLC. Third, RDCA must handle occasional jitters, such as straggler data and burst arrivals of data with a longer post-NIC timespan. We design *Jet*, a cache-centric service tackling these challenges with three key components:

**A cache-resident buffer pool (§4.1).** To address the QP buffer space challenge, we design a cache-resident buffer

pool that uses (1) SEND/RECEIVE verbs and a shared receive queue (SRQ) for receiving small messages, and (2) the READ verb with a window-based rate control mechanism for receiving large messages, so that the total QP buffers can fit into the reserved LLC.

**A swift cache recycle controller (§4.2).** To consume a smaller LLC, we design a swift cache recycle controller that reduces data’s post-RNIC timespan by (1) processing data in parallel along a pipeline and (2) optimizing processing using hardware offloading and lightweight (de)serialization.

**A cache-pressure-aware escape controller (§4.3).** To handle occasional jitters, the escape controller monitors the usage of reserved LLC and takes corresponding actions, including (1) replacing the cache buffer used by straggler data with a new one; (2) copying the data of slow-running applications to memory if there are too many replacements; and (3) let the RNIC mark explicit congestion notification (ECN) in Congestion Notification Packets (CNPs) to indicate congestion if copying to memory fails or cannot release the cache pressure.

**Implementation and evaluation (§5, §6).** We evaluate *Jet* extensively in testbed and production DCN using production storage workloads. *Jet* consumes a 12 MB LLC (20% of the total cache) per server and improves network throughput by up to 2.1x and P99 latency by up to 86.4%. We also evaluate *Jet* in a DCN testbed hosting HPC workloads and find that it reduces the average latency of collective communications in latency-sensitive HPC applications by up to 35.1%.

## 2 Motivation

We first present our measurement study on the receiver host datapath in a production DCN (§2.1). We then elaborate on the rationale and challenges of RDCA (§2.2).

### 2.1 Measurement in a Production DCN

The production DCN consists of multiple Clos-based, IP-based sub-DCNs connected to regional gateways. Each has different hardware and runs RoCEv2 and TCP concurrently. Like other DCNs, the majority workload is storage [14, 37].

**Intermittent receiver throughput drops due to the memory bandwidth bottleneck at the receiver host datapath.** We first investigate a 96-server, two-tier pod in a *PFC-enabled* sub-DCN (*i.e.*, running DCQCN [13] and PFC [38]). Each server has a dual-port 25 Gbps ConnectX-4 LX RNIC. During its operation, we observe intermittent, long-lasting throughput drop (*i.e.*, up to ~15% server throughput drop over 30 minutes). We analyze the logs and find that the only difference before and after the throughput drop is the occupied memory bandwidth at the server.

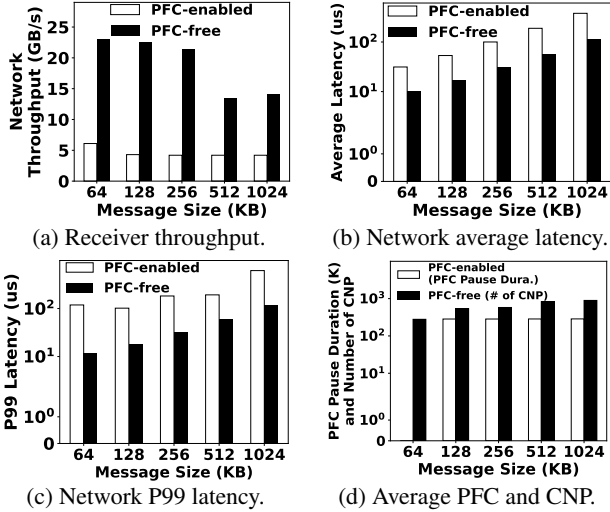


Figure 2: Testbed: network performance under memory bandwidth bottleneck.

We pick one such incident, during which the server’s workload has an approximately 1:1 read/write ratio. Figure 1a shows that it consumes a close-to-capacity  $\sim 60$  GB/s memory bandwidth during the incident. The red line in Figure 1a plots the PFC pause duration of the server during the incident. We observe that the average PFC pause duration is around 80K, with several severe bursts exceeding 100K. Such high PFC pause duration causes the watchdog to frequently trigger PFC switch-off, leading to the server throughput drop.

This throughput drop consistently happens in all sub-DCNs. To be concrete, we next study a pod of the same scale in a *PFC-free* sub-DCN (*i.e.*, running only DCQCN), where each server has a memory bandwidth capacity of 250 GB/s and a dual-port 100 Gbps ConnectX-6 DX RNIC. In another incident, Figure 1b shows that the server consumes a  $\sim 230$  GB/s memory bandwidth and bursts of CNPs are generated by the ECN feature supported in ConnectX-6 DX. This feature detects the watermark of the buffer inside the RNIC and actively sends CNPs as congestion signals to the senders to avoid packet loss caused by the buffer overflow. The throughput drop is therefore a direct result of this large number of CNPs. These bursts of CNPs also happen in another incident in a 25 Gbps PFC-free sub-DCN (Figure 1c). Although we do not have a 100 Gbps PFC-enabled sub-DCN due to its severe PFC storm [9, 13], we believe our observation on memory bandwidth being the bottleneck also holds in such a setting.

**Why receiver memory bandwidth becomes the bottleneck?** To fully understand the reasons behind our findings, we conduct a controlled measurement study on a small testbed with the same hardware and software settings as in the production DCN. We find that the root cause of this bottleneck is the high contention of memory bandwidth among RNIC and CPU cores. Because the RNIC cannot acquire sufficient memory bandwidth to send received messages to memory, in-flight messages queue up in the RNIC buffer and eventually are dropped. Consequently, network congestion control is

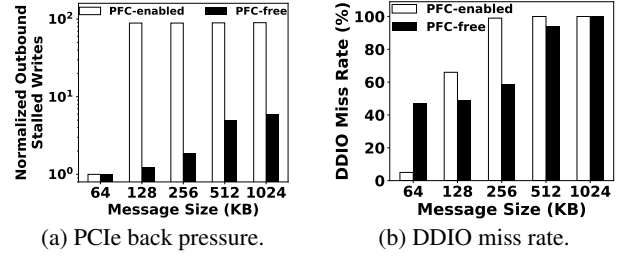


Figure 3: Testbed: PCIe back pressure and DDIO miss rate under memory bandwidth bottleneck.

triggered, resulting in a substantial drop in receiver throughput and a considerable increase in latency. Moreover, we find that instead of alleviating this issue, the state-of-the-art direct cache access technique (*i.e.*, DDIO) could even worsen the situation. Specifically, we consider two scenarios:

- **A 2 \* 25 Gbps PFC-enabled network:** two servers interconnected with a ToR switch. Each server is equipped with PCIe 3.0 \* 8 and a dual-port 25 Gbps ConnectX-4 LX RNIC and enables DDIO with 4 MB cache ways.
- **A 2 \* 100 Gbps PFC-free network:** two servers interconnected with a ToR switch. Each server is equipped with PCIe 4.0 \* 16 and a dual-port 100 Gbps ConnectX-6 DX RNIC and enables DDIO with 6 MB cache ways.

We let one server play the sender to send data with 32 QPs to another server through RDMA `ib_write_bw`. We vary the message size to change the memory footprint of each QP. We simulate CPU cores’ memory bandwidth consumption using RDT *membw* [39], which generates memory bandwidth by reading and writing the memory of 128 MB chunks at a certain frequency. If there is no network activity, *membw* will occupy all available memory bandwidth. We use NVIDIA `neohost` [40] to measure the number of cycles that the PCIe unit had outbound posted write requests but could not operate. We call it the PCIe outbound stalled writes and use it to measure the pressure PCIe brought on RNIC.

We measure how effective DDIO is in alleviating the receiver memory bandwidth bottleneck. We use Intel Performance Counter Monitor (PCM) [41] to count the numbers of PCIe write hit/miss, which reflects the occurrence of DDIO write updates / allocate. More write updates are desirable because it means that RNIC can frequently write data to the cache without swapping it between cache and memory. In contrast, a higher occurrence of write allocate indicates otherwise and hence is not desirable [34, 35].

**Receiver throughput drops and latency increases under high memory bandwidth contention.** Figure 2 plots the receiver throughput, latency, and the corresponding PFC pause duration/CNP in our experiments. Specifically, the receiver throughput/latency decreases/increases as the message size increases. In the 1-MB message size setting, in the PFC-enabled and PFC-free network, the throughput drops by 43.2% and 43.1%, respectively, to that in the 64-KB setting. The increase in average and P99 latency is 11.1x/5.1x and 9.8x/8.9x, re-



spectively. Meanwhile, the PFC pause duration and CNP significantly increase as the message size increases.

**PCIe poses severe back pressure on the RNIC.** Figure 3a shows that the normalized PCIe outbound stalled writes over the 64-KB message setting increase when the message size increases. This indicates that the high memory bandwidth contention leads to severe back pressures from PCIe to the RNIC, which prevents the RNIC from getting sufficient memory bandwidth and eventually causes it to drop overflowed messages. This back pressure is smaller in the PFC-free network than that in the PFC-enabled network. This is because PCIe 4.0 \* 16 is more redundant for a 200 Gbps network capability and confirms that the root cause of our observed performance degradation is insufficient memory bandwidth, not the slow receiver problem [10].

**DDIO does not help under high memory bandwidth contention.** One may expect DDIO should alleviate the high contention on memory bandwidth between the RNIC and CPU cores because DDIO allows the RNIC to access the cache for faster message processing. However, we find that it is not the case. Figure 3b plots the DDIO miss rate (*i.e.*, the frequency of DDIO write allocate). As the contention on memory bandwidth becomes higher (*i.e.*, the message size increases), the DDIO miss rate also increases. When the message size is 1 MB, the miss rate becomes 100% in both networks. This means that every RNIC’s attempt to access the cache will trigger a write allocation, leading to the leaky DMA problem [34, 35]. This is because a larger message size requires the RNIC to reserve a larger space in the cache, which, when added together, exceeds the DDIO-allocated cache. As a result, the RNIC needs to consume an even higher memory bandwidth to operate memory writeback when evicting cache lines for performing DDIO write allocate. A strawman solution one may think of is to allocate a larger LLC for DDIO. However, in our evaluation (§6), we find that even if we double the LLC for DDIO, the receiver still experiences the same throughput drop and latency increase.

## 2.2 RDCA: Rationale and Challenges

Our proposal to cope with the memory bandwidth bottleneck is to move memory out of the receiver host datapath, and reserve a small area in the LLC to let the RNIC access data directly in the cache (*i.e.*, RDCA). The rationale behind RDCA is three-fold. First, the cache has a much higher bandwidth than the memory. Removing the slowest link from the datapath follows the basic principle of optimizing system performance.

Second, RDCA is feasible. Our study in a production DCN shows: after the data leaves the RNIC, no matter if it is sent to a persistent storage media (*e.g.*, SSD), a different processor (*e.g.*, GPU), or consumed by computation tasks (*e.g.*, ranking and counting), the time it spends in memory is usually very short (*e.g.*, hundreds of  $\mu$ s in both average and 99% quantile in our production DCN). As such, from Little’s law [29],

the average amount of data the RNIC needs to store in the memory temporally is small enough to be held in the LLC of commodity server CPUs. For example, for an average post-RNIC timespan of 200  $\mu$ s, we only need a 5 MB space on average to support RNIC operation at 200 Gbps.

Third, RDCA is scalable. The speed of RDMA bandwidth expansion is slower than that of the LLC capacity expansion. RDMA bandwidth increases 4 times in 5 years (100 Gbps/port in 2016 to 400 Gbps/port in 2021). The LLC capacity has increased over 30 times in 9 years (20 MB in Intel Xeon E5 [42] in 2012 to 768 MB in AMD 3rd-gen EPYC in 2021 [43]) As such, we foresee an efficient RDCA implementation requires no substantial redesign in the future.

**Challenges in realizing RDCA.** We identify three key challenges in realizing the RDCA architecture.

- **The mismatch between the small size of reserved LLC and the inefficient reservation of RDMA QPs.** RDMA QPs usually over-reserve large buffer spaces. This leads to inefficient statistic multiplexing of the reserved LLC and compromises the potential benefits of RDCA. As such, we need to improve the level of statistic multiplexing of the reserved LLC among RDMA QPs.
- **The mismatch between reservable LLC and reserved LLC.** Reserving too much LLC for RNIC could cause a higher contention for the remaining LLC among other processes, impairing their performances. As such, it is desirable to reserve a smaller area of LLC while still supporting the RNIC processing received data at line rate. Since the line rate is a fixed value, we need to design techniques to reduce the post-RNIC timespan of data.
- **The mismatch between the reserved LLC and occasional jitters.** The reserved LLC can hold data with an average post-RNIC timespan. However, to ensure that the network can consistently provide high performance, we must take measures to cope with occasional jitters, such as straggler data or burst arrivals of data with a longer post-RNIC timespan.

Next, we present *Jet*, a cache-centric receiver service that realizes RDCA by addressing these three challenges.

## 3 Jet Overview

This section presents the architecture and the basic workflow of *Jet* (Figure 4), a cache-centric service realizing RDCA.

### 3.1 Architecture

*Jet* is a receiver-side service between applications and the RNIC with three key components: a cache-resident buffer pool, a cache-recycle controller and an escape controller.

**Cache-resident buffer pool.** This buffer pool is a reserved area in the LLC that temporally stores the data leaving RNIC. Specifically, to cope with the large space needed by different RQs, it uses an SRQ buffer to receive small-size messages sent using RDMA SEND, and a READ buffer equipped with a window-based rate control mechanism to receive large-size messages sent using RDMA READ.

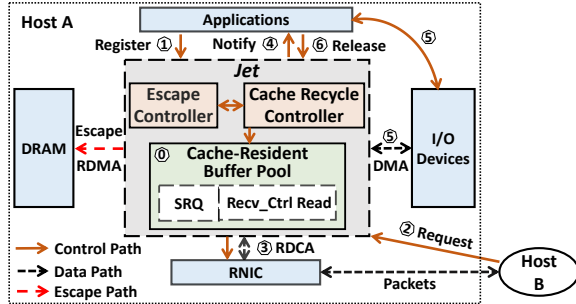


Figure 4: The basic architecture and workflow of *Jet*.

**Cache recycle controller.** This controller is responsible for recycling the cache-resident buffer to temporarily store post-NIC data of different QPs. We develop data processing techniques such as multi-thread, pipeline, hardware offloading and struct-based (de)serialization to reduce the post-NIC timespan of received data, so that *Jet* can multiplex a smaller reserved LLC to support RNIC processing messages at line rate.

**Escape controller.** This controller is responsible for monitoring the usage of the cache-resident buffer pool and taking corresponding actions to handle occasional jitters. It replaces the cache buffer of straggler data with a new buffer, copies the data of slow-running applications to memory if too many replacements happened, and lets the RNIC mark ECN in CNPs to indicate congestion if copying to memory fails or is not sufficient in releasing the cache pressure.

### 3.2 *Jet* Workflow

We illustrate the basic workflow of *Jet* using an example of an application at host A receiving data from host B and writing it to the SSD. Suppose host B wants to send a large chunk of data using RDMA READ. The process is as follows.

**Step 0: *Jet* reserves cache at initialization.** When *Jet* starts, it reserves a space in LLC as the cache-resident buffer pool. It consists of an SRQ buffer for small-size messages and a READ buffer for large-size messages.

**Step 1: application at A registers the *Jet* service.** When the application at A wants to use the *Jet* service, it first registers with *Jet*. If *Jet* grants the registration, it becomes a proxy for the application to receive data and establishes a shared cache mapping between itself and the application. This mapping will later be used to store the metadata of the data RNIC sends to the cache-resident buffer pool.

**Step 2: host B sends *Jet* a request to transmit data using READ.** B constructs a queue pair (QP) with *Jet*. It then sends *Jet* the corresponding metadata, such as the data size and the memory address at B. Upon receiving such a request, the cache recycle controller adds it to an admission queue and processes receive requests in the queue in a first-in-first-serve order. A request is granted if (1) the expected cache footprint of the request (*i.e.*, the expected throughput of the request times its expected post-NIC timespan) is smaller than the remaining capacity of the cache-resident buffer pool, and (2) the number of concurrent transmissions in *Jet* is below a pre-defined threshold. Once the request is admitted, *Jet* allocates

an area in the READ buffer for this request.

**Step 3: *Jet* forwards the admitted request to RNIC for data transmission.** After allocating the corresponding area in the cache-resident buffer pool, *Jet* forwards the request to the RNIC as well as the cached address to which the RNIC can send the received data. The RNIC receives this request and starts to retrieve the data from the memory of host B.

**Step 4: *Jet* notifies the application once data arrives at the cache.** When the RNIC receives the data, it forwards them to the cached address in the cache-resident buffer pool specified in Step 3. The cache recycle controller notifies the application process about the arrival of data with the pointer to the corresponding address through the shared cache mapping established in Step 0.

**Step 5: the application writes the received data to SSD.** When receiving the notification from *Jet*, the application sends SSD a pointer to the cached address of the data. SSD uses this pointer to retrieve the data from the cache-resident buffer pool using DMA. Step 4 and 5 continue until the whole data from B is written to the SSD at A.

**Step 6: *Jet* releases the allocated cache when notified by the application.** After finishing the data writing, SSD notifies the application, which then notifies *Jet* through the shared cache mapping. The cache recycle controller then releases the allocated cache for further use.

If host B sends small-size messages to A using RDMA SEND, the workflow stays the same except for Step 2 and 3: when constructing the QPs, *Jet* posts work queue elements (WQEs) to the SRQ, binds them with a cache area in the SRQ buffer and sends the RNIC the cached address. Instead of sending a request first, host B directly sends the data to *Jet* and the RNIC sends the received data to the corresponding cache area.

Suppose an application does not write the received data to SSD, but instead sends them to another processor (*e.g.*, GPU) or performs in-memory computation (*e.g.*, ranking). Step 5 and 6 of the workflow also change correspondingly.

## 4 *Jet* Design Details

We now present the details on how *Jet* addresses the three challenges in realizing RDCA (§2.2).

### 4.1 Cache-resident Buffer Pool

We design the cache-resident buffer pool to address the mismatch between the small size of reserved LLC and the inefficient reservation of RDMA QPs by limiting the memory buffer used by the received data. Specifically, we adopted different RDMA operations and control methods for small and large messages respectively. For small messages, we choose the RDMA SEND/RECEIVE, together with SRQ mechanism to aggregate RQs. For large messages, we use RDMA READ, together with a *receiver-side read control mechanism* to limit the number of concurrency and the size of in-flight messages (*e.g.*, messages in transit).

#### 4.1.1 Small Messages: SEND/RECEIVE With SRQ

**Using SEND/RECEIVE for low latency.** We choose the RDMA SEND/RECEIVE operation to transmit small messages (*i.e.*, messages smaller than 4 KB). Because small messages are latency-sensitive and require low-delay transmission. While SEND/RECEIVE takes one RTT time less than READ when transmitting messages. However, if every QP utilizes its own RQ exclusively, it may take up a lot of memory footprint. Since in order to prepare for receiving a large number of burst messages, a sufficient number of WQEs need to be posted into the RQ [44] in advance. These WQEs require to have MRs (Memory Regions) registered in the memory and take up memory footprint. Thus, too many WQEs would cause the size of the memory footprint to be larger than the capacity of the cache. Besides, not all the QPs are active usually, which makes the utilization of WQEs and their pointing memory footprint very low.

**Using SRQ to aggregate RQs.** In order to reduce the required size of the memory footprint, we use the SRQ [45] to aggregate RQs. Specifically, SRQ allows multiple QPs to share one RQ, decreasing the required number of WQEs and cutting down the size of the memory footprint. When any QP receives a message, the hardware will extract a WQE from the SRQ, and store the received data according to the address provided by the WQE. Then, completion information would be returned to the corresponding upper user through the completion queue. Since SRQ can reduce the number of WQEs that need to be posted, SRQ is conducive to reducing the size of the memory footprint so that it can reside in the cache and ensure that burst messages can be handled.

#### 4.1.2 Large Messages: Read With Receiver-side Control

**Using READ for high throughput.** We employ the READ to transfer large messages (*i.e.*, messages larger than 4KB). READ helps in avoiding the problem of large message failure because it allows the receiver to decide the address and length of the memory footprint allocated to receive messages. Meanwhile, after obtaining the memory address, length, and key of the remote data, the receiver can directly acquire access to the data in the sender. Therefore, the READ does not require the involvement of the sender software stack and is a unilateral operation, providing high throughput.

**Message fragmentation.** We also fragment large data messages, because the amount of data sent in a single time is unfavorable for flow control. In addition, if the message is lost, the retransmission requires non-negligible overhead. Besides, large messages will be divided into slices in the network transmission. Too many slices are prone to cause the packets out-of-order problems, and arrived packets need to wait for the latest packet and take up the memory footprint. Thus, we slice the messages into no larger than 256 KB fragments before transmitting them.

**Receiver-side control mechanism.** To restrict the memory footprint used by READ, we design the *receiver-side read*

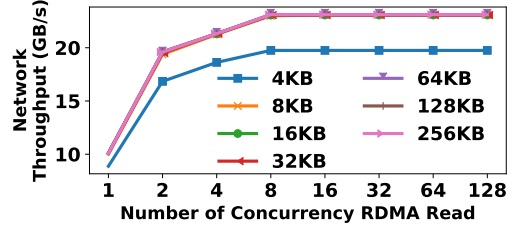


Figure 5: The network throughput of different READ concurrency numbers and message sizes.

*control* mechanism [15, 46], which consists of two parts: concurrency number control, and in-flight buffer size control.

**1. The concurrency number control.** A fixed-size sliding window is maintained to limit the number of admitted READ requests. Only requests that are in the window are allowed to be sent. If there is not enough window capacity, the requests will be waiting in the request queue, which is a first-in-first-out queue. Until the previous requests are processed, the window moves, and then the subsequent requests can be processed. With a fixed-size sliding window, we can control the number of concurrent READ requests to be less than a certain value (*e.g.*, 32). What’s more, this concurrency number control can also help to solve the in-cast problem, which is caused by burst messages arriving at the receiver RNIC simultaneously and would affect the latency and throughput of message transmission [15].

Besides, we do experiments to test how many concurrencies and how large the message size can fully utilize the network bandwidth using a single thread. As the results shown in Figure 5, when the concurrency number equals to four, the 2\*100 Gbps network bandwidth can be fully utilized. Usually, the number of active network connections is 32. Thus, we set the concurrency number 32.

**2. The in-flight buffer size control.** We use another window to limit the total amount of memory footprint taken up by in-flight READ data. Specifically, a fixed-size window (*e.g.*, 8MB) is maintained to bound the dynamic number of inbound bytes. If the available window capacity is less than the size of messages requested by READ, this READ request would be queued and deferred until sufficient window capacity is allocated to the request. When a READ request is processed, its corresponding occupied window capacity can be released for subsequent read requests.

#### 4.1.3 Deciding the size of the cache-resident buffer pool

To ensure that the capacity of the cache-resident buffer pool can meet the requirements of receiving data and is not too large, we take both the message size and concurrency number into consideration carefully to calculate its size. Specifically, for 32 QPs we prepare 1K WQEs in advance in the SRQ to deal with received small messages, and the size of each WQE is 4 KB. Thus, the size of the SRQ buffer is initially set as 4 MB. Considering that the size of the largest message is 256 KB and the READ concurrency number is 32, the READ buffer allocated for big messages is initialized as 8 MB. Note



that the SRQ buffer and the READ buffer share the whole 12 MB space. Thus, the size allocation between the two buffers can be dynamically adjusted at runtime, only guaranteeing that the size of the SRQ buffer is larger than a threshold.

## 4.2 Swift Cache Recycle

In order to eliminate the mismatch between reservable LLC and reserved LLC, we design a *swift cache recycle mechanism* in the cache recycle controller to reduce the required cache size and shorten the time that applications occupy the cache buffer. Specifically, first, we take advantage of the slab [47] algorithm to manage the cache buffer in the granularity of 4 KB. Because the slab algorithm can divide the cache buffer into object pools, solving the problem of internal fragmentation. Second, *Jet* and applications transfer metadata and release requests of cache buffers through shared caches to realize cache buffer recycle. Third, in order to speed up the process of the cache cycle, we have made the following optimizations: (1) use multi-thread to perform data processing operations at the same time and achieve parallelism, (2) leverage pipeline technology to realize cache recycle in finer granularity, and (3) simplify the data process to further improve efficiency and shorten the time.

### 4.2.1 Cache Buffer Recycle

To be specific, in the initialization phase, *shmget* is used to allocate one cache space shared by *Jet* and the application in the cache. Also, *shmat* is used to mount and map this shared space to both *Jet* and the application address spaces. In this way, after getting the received data from RNIC to the cache buffer in the cache-resident buffer pool, *Jet* delivers the address pointer pointing to the cache buffer to the application through shared cache. If the data needs to be further transmitted to the I/O devices, the I/O devices can obtain the data through DMA operation. When the application processes finish receiving and processing the data, they can use the shared cache again to inform *Jet* to release the cache buffer. The occupied cache buffer is released back to the cache-resident buffer pool, which can be used for the subsequent requests, realizing the cache buffer recycle.

### 4.2.2 Accelerating the Recycle

We accelerate the cache buffer reuse rate to guarantee the availability of *Jet* and shorten the timespan data spent in the cache. The relationship between *Jet* and applications can be abstracted as the producer-consumer. *Jet* is responsible for getting the received data into the cache buffer, which plays the role of the producer. While the applications are responsible for using the obtained data from the cache buffer, thus applications can be regarded as consumers. Thus, in order to recycle the cache more quickly, we speed up the rate at which producers produce data through three methods: using multi-thread to achieve data processing parallelism, segmenting data to form a pipeline, and simplifying data processing.

**Realizing processing parallelism through multi-thread.**

Due to the differences between the network software stack and application software stack, data packets received by the RNIC need to be processed by *Jet* first. For example, there are cyclic redundancy check (CRC) checksum, data serialization/deserialization, and data formation. These non-negligible data processing overheads will slow down the speed at which *Jet* provides the data to the applications. Therefore, in order to narrow the gap between the speed of data produced by *Jet* and the speed of data consumed by the application, we introduce multi-thread. These threads can perform data processing operations concurrently to achieve parallelism and shorten the processing time.

**Forming a data processing pipeline.** We use I/O pipeline processing to match the rate between producer and consumer in a finer-grained. Specifically, the timespan in data processing can be roughly classified into three stages: get, process, and release. First, *Jet* gets the data into the cache-resident buffer pool from the RNIC. Then, *Jet* processes the data as needed to meet the requirements of the applications. At last, *Jet* forwards the data to applications and applications notify *Jet* to release the cache buffer. In order to form a data processing pipeline, we segment the data messages into slices no larger than 4 KB [15]. These slices enter the three stages sequentially and continuously, and once the timespan of a slice finishes, the cache buffer it occupied can be released immediately. Thus, there is no need to wait until the application receives the whole message and notifies to release the cache buffer. By forming this small-slice data processing pipeline, we can recycle the cache-resident buffer pool more efficiently.

**Simplifying the data processing procedure.** What's more, we simplify the processing software and offer a simpler way to (de)serialize data as well. First, some data processing tasks can be offloaded to dedicated hardware. Take the storage system as an example. The CRC calculation is offloaded to an RNIC with CRC check calculation capabilities (e.g., Mellanox CX-5 [48]), so that *Jet* is not required to calculate the CRC and thus save data processing time [9]. Second, we provide a compiler that can (de)serialize data for remote procedure call using *huibuffer* [49], a lightweight data serialization protocol. Specifically, serialization and deserialization are data conversion technologies. Serialization is to reorganize the data according to the specified format while keeping the original data semantics unchanged. Deserialization is to restore the serialized data to semantic data and regain the original data. Unlike *protobuf* [50] which needs memory copy and uses objects in (de)serialization, *huibuffer* can achieve in-place (de)serialization and use struct. *Huibuffer* has the advantages of flexibility and high performance.

## 4.3 Cache Pressure-Aware Escape Mechanism

An escape mechanism, which perceives the cache pressure and adjusts actively, is designed to deal with the mismatch between the reserved LLC and occasional jitters (e.g., SSD

---

**Algorithm 1:** The escape algorithm.

---

```
1 Function escape()
2   // The cache pool is insufficient.
3   if avl_cache_pool < CACHE_SAFE then
4     // The memory size for escape is small.
5     if replace_mem_size < MEM_ESC then
6       // Replace straggler buffers.
7       buffer_replace();
8     else
9       // The escape memory size is large, the data of
10      // slow-release applications needs to be copied
11      // to memory.
12      foreach app_id do
13        // Most cache buffer of app_id is straggler.
14        if  $\frac{\textit{straggler\_buf\_num\_id}}{\textit{held\_buf\_num\_id}} > \textit{CREDIT}$  then
15          // Copy data to memory by
16          // multi-thread.
17          data_copy(app_id);
18      // Data copy does not work because of exceptions.
19      if avl_cache_pool < CACHE_DANGER then
20        mark_ecn();
21  else
22    // The cache pool is enough, do not need to escape.
23    Do nothing;
```

---

slow write, and application exceptions). Specifically, when there is not enough capacity for the slab to allocate buffers in the cache-resident buffer pool, it means the pressure of the cache is too high. In this case, the escape controller will trigger this mechanism as a safety net. Our evaluation (§6) shows that the probability of it being triggered is very low.

**Escape algorithm.** The escape algorithm is summarized in Algorithm 1. There are five parameters in this algorithm: *CACHE\_SAFE* and *CACHE\_DANGER* measures the usage of the cache-resident buffer pool usage, *MEM\_ESC* measure the size of memory used for escape, and *CREDIT* measures whether an application is slowly-releasing. Note that the *CACHE\_DANGER* is lower than the *CACHE\_SAFE*. Besides, there are two main variables. *held\_buf\_num\_id* represents the total number of buffers occupied by application numbered *id*. If the time an application occupies the cache buffer is greater than a time threshold, the cache buffer will be considered a straggler buffer. The number of straggler buffers occupied by application numbered *id* is recorded as *straggler\_buf\_num\_id*. For an application numbered *id*, if the value of *straggler\_buf\_num\_id* divided by *held\_buf\_num\_id* is greater than *CREDIT*, the application is considered to be a slowly-releasing one. To add, the cache buffer allocated for each application is organized by linked lists. If a new cache buffer is allocated to an application, then a node would be linked to the tail of its linked list. Thus, the timestamp of the cache buffers in a linked list is monotonically increasing. Thus, we can know whether the time of a cache buffer ex-

ceeds the time threshold by checking the timestamp of the head node in the linked list. This method provides a time complexity of  $O(1)$ .

In this escape algorithm, we design three different escape actions to cope with three different degrees of abnormalities. To be specific, when the available size of the cache-resident buffer pool is smaller than *CACHE\_SAFE* and the used memory size for escape is smaller than *MEM\_ESC*, we replace the straggler buffers. Else, for each application whose straggler cache buffers take up more than *CREDIT* percent of total occupied cache buffers, we copy the data belonging to the application from the cache into the memory. The impact caused by copying data to memory on the memory bandwidth is negligible. Since using  $\alpha$  to represent the proportion of influenced flows when escape happens, the added memory bandwidth consumption equals at most to  $\alpha \times \textit{network\_bandwidth}$ . Considering the extreme situation where the network throughput is 100 Gbps and  $\alpha$  is 4%, the memory bandwidth only increases at most by 1 GB/s.

However, copying data from the cache to memory may do not work due to some exceptions, such as machine check exception [51]) which is the hardware error in the processor, cache, memory, or system bus. In this scene, the available size of the cache-resident buffer pool becomes lower than *CACHE\_DANGER*. To solve this problem, we mark ECN in CNPs to indicate congestion in the receiver datapath and slow down the data-sending rate.

**Replacing straggler buffers.** In this escape action, we simply do not use the straggler buffer for cache recycling. Instead, an extra buffer of the same size is allocated in the memory and pre-touched, joining the cache-resident buffer pool for recycling. In this way, the total size of the usable and recyclable cache-resident buffer pool remains unchanged. A background task is responsible for replacing the straggler buffer which reads the memory footprint sequentially and periodically at a low frequency.

**Copying the data to the memory.** In this escape action, we copy all the data in cache buffers occupied by slowly-releasing applications into the memory. By doing this, the straggler cache buffer can be released quickly. Copying the data to the memory will not consume extra memory bandwidth (since using RDMA also needs memory bandwidth), and can guarantee that the packets received from the network would not be dropped due to memory bandwidth bottleneck. Because copying the data from cache to memory is initiated by the CPU instead of RNIC, and in the allocation of memory bandwidth resources, the CPU has higher priority than the RNIC. In this way, we can fully utilize the network bandwidth which is more precious than the memory bandwidth.

**Marking ECN.** The enhancement of hardware capabilities enables the RNIC to handle more complex tasks and functions, including marking ECN in CNPs. Although marking ECN is a new function of the latest RNICs (e.g., ConnectX-6 DX [52]), previous models of RNICs can also implement



such a function by adding firmware. Thus, we mark ECNs to indicate the available size of the cache-resident buffer pool is below `CACHE_DANGER`. By doing this, the sender would slow down the speed of sending data when receiving CNPs, alleviating the pressure on the cache on the receiver. In our experiments, this mechanism is barely triggered.

## 5 Implementation

We implement a prototype of *Jet* in 7K C code and deploy it in commodity servers. We encounter three practical issues. **Cache isolation: a problem with CAT.** We use the Cache Allocation Technology (CAT) [53] to reserve a dedicated LLC for *Jet*. However, we find that data in the reserved cache can be swapped out even when the RNIC is not receiving data at line rate. We identify two reasons. First, both the code of *Jet* and the host network stack compete for the reserved cache. As such, the data could be forced out by the code. We address this by slightly increasing the reserved cache size and periodically touch random data in the buffer pool. Second, scheduling mechanisms in operating systems (e.g., cache prefetching) could cause other data to occupy *Jet* reserved cache. As such, we turn off these functions during deployment. In our evaluation, we find that doing so does not affect the overall application performances.

**Marking ECN without corresponding RNIC interfaces.** The last resort of the escape controller is to let RNIC mark ECNs in CNPs. However, the ConnectX RNICs on our servers do not provide interfaces to send CNPs. We workaround this limitation by using a provided interface to adjust the ECN marking threshold of the RNIC: lower the threshold when the cache buffer is being exhausted so that the RNIC can start to send CNPs, and resume it when the available cache buffer is above the safety line. Although the adjusting ECN threshold takes time and is a seldom taken action in daily DCN operation, we do not expect to activate this action frequently in *Jet*, but treat it as a safe net. In fact, in our evaluation, we observe very rare activation of this action.

**Guaranteeing application QoS.** We implement admission queues with different priorities. Applications with higher QoS level is admitted access to *Jet* cache pool with a higher priority. If there is no available cache buffer for an application with low QoS level, *Jet* will let them use memory buffer instead.

## 6 Performance Evaluation

We evaluate *Jet* in different networks that differ in scale, RNICs, CPUs and workloads. We compare *Jet* and the default data packet processing design (DDIO) in the experiments. We aim to evaluate the effectiveness of all designs in *Jet* (§ 6.1), the application-level effectiveness (§ 6.3), and the generality of *Jet*. (§ 6.4)

### 6.1 Experimental Setup

**Testbed setup.** The testbed contains two hosts: one client and one server. Both hosts are deployed with *Jet*. We use two testbeds in § 2.1: the 2 \* 25 Gbps PFC-enabled network

and the 2 \* 100 Gbps PFC-free network. We compare *Jet* with DDIO. For fairness, we allocate 12 MB LLC for DDIO and *Jet* (4 MB for small messages and 8 MB for large messages (§4.1)) in both networks. We run a synthetic storage benchmark provided by a major cloud provider, which simulates the process of its production DCN except that data will not be written into the SSDs. We configure the tool to produce messages with sizes between 4 KB and 256 KB.

**Production DCN.** We conduct experiments on the disaggregated storage architecture, which includes a storage cluster and a computing cluster. The storage system consists of 16 hosts. For high availability, each host is configured with a dual-port Mellanox RNIC connected to 2 ToR switches. These ToR switches are connected through spine switches. The topology is a typical Clos network, which is widely adopted in real data centers. Note that we run RoCE RDMA without TCP. In this cluster, we use the same configured hosts as the second testbed in §2.1. Each host is equipped with 12 SSD and 2 Optane SSD. In this cluster, we also configure *Jet* with 4 MB LLC for small messages and 8 MB LLC for large messages (§4.1). For fairness, DDIO also uses 12 MB LLC. The computing cluster has another 16 hosts. These hosts send three sizes of messages: 4 KB, 16 KB, and 256 KB, where the messages are produced with the modified FIO [54], which is a program that can set flexible workloads for I/O performance tests. We randomly select a host to measure its performance, given that the performance is similar across hosts.

### 6.2 Testbed Micro-benchmark Experiments

The micro-benchmark evaluates and validates the designs in *Jet* separately. We first measure the macro metrics to show the overall performance. Under this premise, we explore its inner mechanisms via the micro metrics.

**Throughput.** Figure 6a and 7a show the results of network throughput results. Overall, the network throughput of *Jet* outperforms the baseline and achieves up to 1.96x throughput. Compared with the baseline, *Jet* with cache isolation and cache-resident buffer pool achieves 1.96x and 1.54x throughput in PFC-free networks and PFC-enabled networks with a 256 KB message size, respectively. Compared with the baseline, cache isolation improves network throughput by 5% and 2.6% for PFC-free networks and networks with PFC on the 256 KB message size. This reveals that *Jet* can improve the throughput via bypassing the memory bandwidth bottleneck.

**Network latency.** The experimental results of network latency are shown in Figure 6b and 7b. As we can see, *Jet* achieves low latency in both networks, especially in the PFC-enabled network. In the PFC-enabled network, *Jet* improves the network delay of small messages (4 KB) by 46.4%; the 256 KB messages' delay is improved by 74.8%. In the PFC-free network, the performance improvement of *Jet* is more significant. In these three designs, the cache-resident buffer pool has the most significant improvement on the latency of the PFC-enabled network and the PFC-free network. The

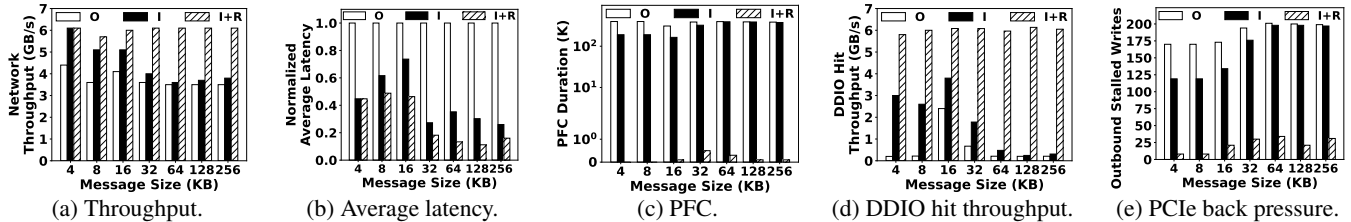


Figure 6: Micro-benchmark experiment results on the dual-port 25 Gbps PFC-enabled RDMA network. In this figure and the following figures, ‘O’ indicates the DDIO’s performances, and ‘I’ and ‘R’ means the performance with the cache isolation and the cache-resident buffer pool, respectively.

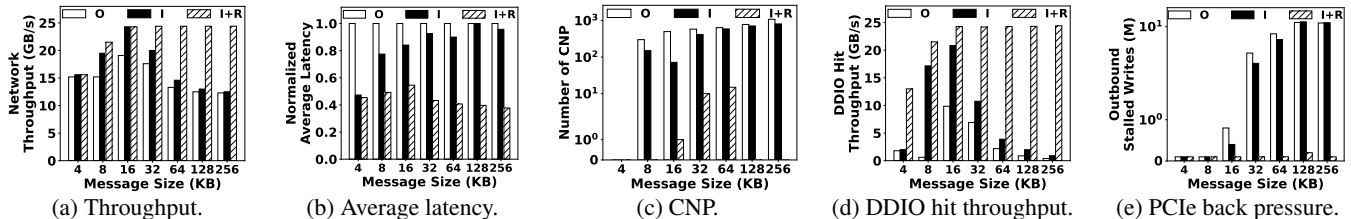


Figure 7: Micro-benchmark experiment results on the dual-port 100 Gbps PFC-free RDMA network.

reason is that *Jet* can efficiently use cache.

**PFC and CNP.** We measure the PFC duration of the PFC-enabled networks and the number of CNP of the PFC-free networks for fine-grained analysis of network throughput. In summary, *Jet* with the cache isolation and the cache-resident buffer pool could almost remove PFC pause frames and CNP packets, and guarantee high throughput (Figure 6c and Figure 7c). Specifically, for the PFC-enabled networks, *Jet* can make the network not affected by memory bandwidth bottleneck, and avoid buffer accumulation and PFC generation. Figure 6c shows for the PFC-enabled networks, the PFC duration of *Jet* is almost 0 for different network messages. In addition, as shown in Figure 7c, the number of CNP of *Jet* is also close to 0 for most network messages (except for 32 KB and 64 KB messages). This indicates that *Jet* can bypass memory bandwidth bottlenecks and guarantee network performance.

**DDIO hit throughput.** DDIO hits mean DDIO write update is triggered. DDIO hit throughput under the different network messages as shown in Figure 6d and Figure 7d. This means the network throughput of DDIO writes an update (aka. cache hits throughput). The improvement of DDIO hit throughput is notable. Compared with the baseline, *Jet* performs 56.6x and 26.7x DDIO hit throughput for PFC-free networks and the PFC-enabled networks for 256 KB network messages under the memory bandwidth bottleneck. The reason is that as the network message size increases, the required memory footprint size also increases, increasing the probability of cache conflicts. *Jet* can achieve a high cache hit ratio and liberate from the memory bandwidth bottleneck.

**PCIe back pressure.** We study the PCIe back pressure in *Jet* in Figure 6e and Figure 7e. Compared with the baseline, *Jet* reduces the PCIe outbound stalled writes by up to 99.1% and 96.4% for the PFC-free networks and the PFC-enabled networks for the 256 KB network message under the memory bandwidth bottleneck, respectively. The reason is that *Jet* can process the network messages in the LLC directly and avoid

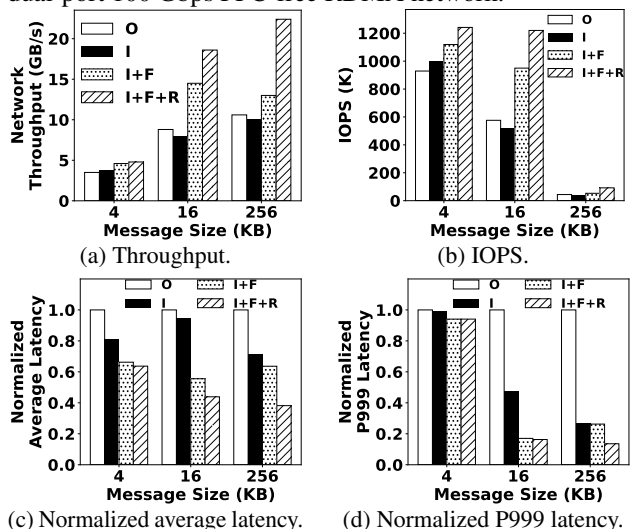


Figure 8: The performance results of *Jet* and the default design, where ‘F’ means the adaptive cache evacuation.

touching the memory. With the efficient data paths, *Jet* is free from memory bandwidth competition.

### 6.3 Production Storage Workload in Production DCN

We evaluate *Jet* and the compared methods on multiple macro metrics. Since the three designs of *Jet* optimize the performance incrementally, we also evaluate the performance of their incremental combinations in Figure 8. We also measure and analyze the running cache and memory of *Jet*.

**Throughput.** Figure 8a shows that compared to the baseline, the CAT cache isolation of *Jet* achieves almost the same network throughput with a slight drop for network messages of three sizes. The reason is that the cache isolation reduces the cache used by the network thread, and improves the probability of cache conflict inside the network buffer. The CAT cache isolation and cache evacuation of *Jet* achieve better

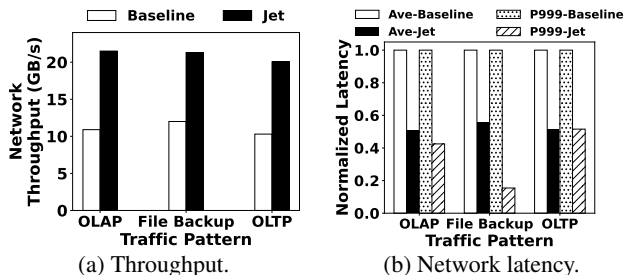
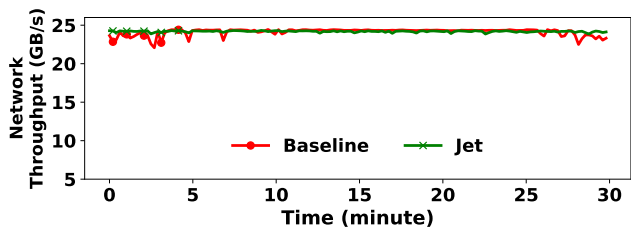


Figure 9: The *Jet* performance in different storage workloads. performance compared with the baseline on 4 KB, 16 KB, and 256 KB messages, respectively. With these three designs, *Jet* improves the throughput by 2.11x for both 256 KB messages and 16 KB messages. This shows that *Jet* can fill the performance degradation gap of isolation and improve the overall throughput.

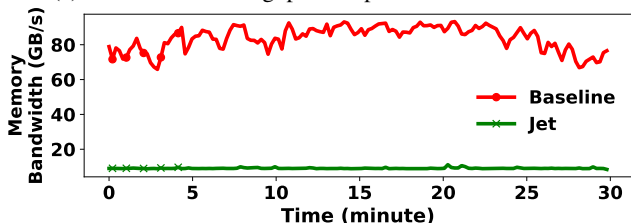
**IOPS.** Figure 8b shows that the IOPS of *Jet* outperforms the baseline at network messages of three sizes. Compared to the baseline, cache isolation reduces the IOPS for large messages (256 KB) by 5.7% and middle messages (16 KB) by up to 10.4%. This reason is the data ping-pong between memory and cache improves latency due to the cache collision. Compared with cache isolation, after integrating fast cache recycle, network messages can be stored in the SSDs at a higher speed, which reduces the probability of cache collisions. The experimental results reveal that the two designs can improve 20.5% and 64.8% IOPS compared to the baseline for large and middle messages, respectively. By continuing to integrate the cache control, *Jet* increases 109.1% and 111.4% IOPS for large and middle messages. This shows *Jet* can benefit the network messages of storage on IOPS.

**Latency.** The experimental results of network delay are shown in Figure 8c and Figure 8d. We can conclude that the isolation has some influence on the average network latency, whether the size of network messages is 4 KB, 16 KB, or 256 KB. Cache evaluation and cache-resident buffer pool can greatly reduce the average and P999 network latency. For example, with the three designs, the average latency of 16 KB messages decreases by 43.5% and the average latency of 256 KB messages decreases by 51.6%. The P999 latency of 256KB messages decreases by 86.4%. This reveals the effectiveness of the cache control mechanism.

**The performance of *Jet* under different real traffic patterns.** We evaluate the performance of *Jet* with different real traffic loads on one of the hosts in the cluster. Specifically, we use three traffic patterns of distributed storage systems: OLAP (online analytical processing), File Backup, and OLTP (online transaction processing), which are monitored and abstracted from the trace of a five-year large-scale cloud storage system. Each traffic pattern is a collection of messages whose size is controlled within a range. We use FIO on one computing node to produce the traffic loads and send them to the storage node. Figure 9a and Figure 9b show the throughput and latency results under different traffic patterns.



(a) The network throughput comparison for 30 minutes.



(b) The used memory bandwidth comparison for 30 minutes.

Figure 10: The memory monitor of *Jet* without the memory bandwidth pressure.

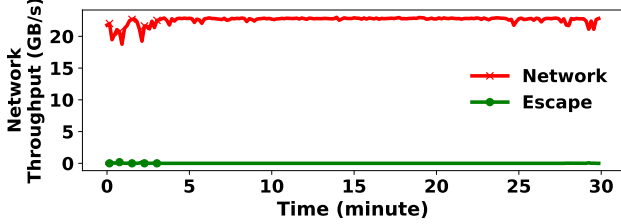
We can conclude that *Jet* improves the throughput by up to 1.97x and reduces the average latency by up to 1.97x on all the traffic patterns. The consistent performance improvement demonstrates the efficacy and efficiency of *Jet*.

**The used memory bandwidth of *Jet*.** We also measure the memory bandwidth consumption of *Jet*. As shown in Figure 10a, *Jet* improves network throughput by up to 4.5% on average. We can see that *Jet* decreases nearly 89% memory bandwidth consumption on average from Figure 10b. The memory bandwidth consumed by *Jet* is mainly from the escape mechanism. It is worth noting that the memory bandwidth used by the escape mechanism is less than 0.5 GB/s. In summary, *Jet* uses small memory bandwidth to maintain stable network throughput. It reveals the effectiveness of the escape mechanism. Furthermore, *Jet* can reduce network throughput and memory bandwidth jitters. This is because with *Jet*, RNICs can directly write data to the cache and data is forwarded to the SSDs, reducing the number of memory accesses.

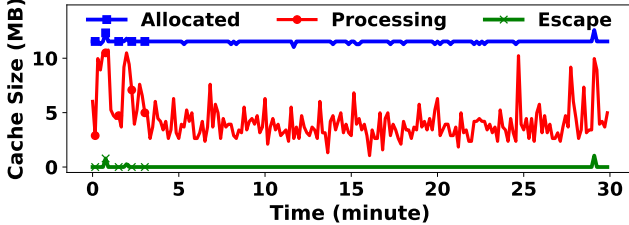
**The used cache of *Jet*.** We monitor the used cache of *Jet* to dig into the internal mechanism of the cache in *Jet*. Figure 11b shows the cache usage of *Jet* without the memory bandwidth pressure. The extra cache triggered by the escape mechanism is less than 1 MB. With such a small escape cache, *Jet* achieves a stable network performance. In Figure 11b, the allocated cache and the escape cache are stable except for the start and end. At these two time points, *Jet* triggers the escape mechanism to introduce a cache replacement.

**Storage LLC hit ratio.** We evaluate the LLC hit ratio to analyze the used cache. Figure 12a shows that *Jet* improves the LLC hit ratio. The cache isolation and fast cache recycling of *Jet* achieve 4.18x LLC hit ratio for large (256 KB) messages. *Jet* can achieve 5.06x LLC hit ratio for the 256 KB messages. The reason is that the storage system is not sensitive to data-locality access. *Jet* decouples network threads and storage threads to reduce cache collision. Compared with the baseline, the cache isolation changes little in the LLC hit



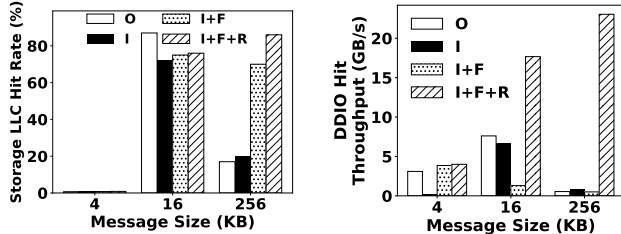


(a) The network throughput of *Jet*.



(b) The used cache of *Jet*, where the processing cache, allocated cache, and escape cache indicate the cache that is being occupied by the storage system, the cache pool, and extra cache triggered by the escape mechanics, respectively.

Figure 11: The cache monitor of *Jet*.



(a) Storage LLC hit ratio.

(b) DDIO hit throughput.

Figure 12: DDIO hit ratio on dual-port 100 Gbps network.

ratio as the allocated cache for storage becomes smaller.

**DDIO hit throughput.** To verify the validity of *Jet*, we also measure the DDIO hit throughput. As shown in Figure 12a, *Jet* achieves the best network throughput. Compared with the baseline, *Jet* achieves 2.32x and 42.4x higher DDIO hit throughput for 16 KB and 256 KB messages under the memory bandwidth bottleneck, respectively. This shows that the DDIO hit of *Jet* in storage applications can perform well as in micro-benchmark.

## 6.4 *Jet* in HPC Workload

We also evaluate the performance of *Jet* on MVAPICH [4], a high-performance programming library collection. We use two hosts in §2.1 to simulate eight computing nodes, where the two hosts are connected with a ToR switch, each host runs four processes, and each process acts as a node. We also configure 12 MB LLC for DDIO and *Jet*, where 4 MB accounts for the small messages and 8 MB accounts for the large messages. We run six MPI benchmarks, and each node produces 4 MB network messages. Figure 13 shows the average latency of *Jet* compared with DDIO. *Jet* reduces the communication latency among all nodes under the pressure of the memory bandwidth bottleneck. For the all-to-all and all-gather communication patterns, *Jet* reduces the latency by up to 35.1% and

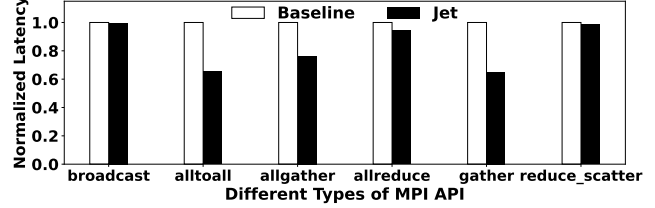


Figure 13: The latency on MPI library benchmark.

25%. For the all-reduce communication pattern, *Jet* reduces the latency by up to 5.5% than the baseline. This reveals that *Jet* can improve the performance of HPC applications.

## 7 Related Work

**RDMA operation optimization.** Many studies optimize RDMA-enabled distributed applications by using programmable RNICs to offload computation [17, 19, 22, 23, 55–58] and designing scalable RPCs to efficiently use RNIC buffers [15, 16, 59, 60]. They are tailored for specific applications or specific RDMA verbs. DC providers design different congestion control algorithms [13–15, 46, 61, 62] to ensure RDMA operation efficiently in large-scale DCNs. They focus on the network fabric congestion and ignore the potential congestion on the receiver host datapath. Some recent studies propose to redesign RNIC by adding memory modules [26–28, 63]. They require upgrading DCN with specialized, non-commodity RNICs. In contrast, we identify that the memory bandwidth bottleneck can cause congestion in the receiver host datapath and propose the RDCA architecture to circumvent it. To our best knowledge, we are the first to identify and tackle this memory bandwidth bottleneck.

**Direct cache access.** DCA [30] and DDIO [31, 32] take the first steps in using LLC for fast packet processing. Their benefit in high-speed networks is small due to the leaky DMA problem [33–36]. Some studies propose to dynamically adjust the LLC allocation in response to the cache pressure to improve the performance of DDIO [18, 34–36]. In our evaluation, we show that even doubling the LLC size for DDIO does not improve its performance in high-speed networks due to the memory bandwidth bottleneck. In contrast, *Jet* fully multiplexes a small area of LLC to achieve efficient RDCA, enabling high throughput and low latency under memory bandwidth bottleneck.

**Congestion in the receiver host datapath.** Our private conversations with other DC operators show that the memory-bandwidth-induced congestion in the receiver host datapath is not an isolated finding. One operator recently publishes about this issue without proposing a solution [20]. In contrast, we propose and implement the RDCA architecture that addresses this issue with success.

## 8 Conclusion

We identify the memory bandwidth as the bottleneck of the receiver host datapath of RDMA. To cope with it, we propose the RDCA architecture that lets remote hosts directly access

local cache. We design a service *Jet* that realizes RDCA. Extensive experiments demonstrate its feasibility and benefits. **Acknowledgments.** we are extremely grateful for the wonderful comments from the OSDI'23 anonymous reviewers. The comments are invaluable for improving our manuscript in the next version.

## References

- [1] Satadru Pan, Theano Stavrinou, Yunqiao Zhang, Atul Sikaria, Pavel Zakharov, Abhinav Sharma, Shiva Shankar P., Mike Shuey, Richard Wareing, Monika Gangapuram, Guanglei Cao, Christian Preseau, Pratap Singh, Kestutis Patiejunas, J. R. Tipton, Ethan Katz-Bassett, and Wyatt Lloyd. Facebook's tectonic filesystem: Efficiency from exascale. In *FAST*, pages 217–231. USENIX Association, 2021.
- [2] Sanjay Ghemawat, Howard Gobioff, and Shun-Tak Leung. The google file system. In *SOSP*, pages 29–43. ACM, 2003.
- [3] Lukas Spies, Amanda Bienz, J. David Moulton, Luke N. Olson, and Andrew Reisner. Tausch: A halo exchange library for large heterogeneous computing systems using mpi, opencl, and CUDA. *Parallel Comput.*, 114:102973, 2022.
- [4] Mvapich. <https://mvapich.cse.ohio-state.edu/> / Accessed Dec 12, 2022.
- [5] Kamalakant Laxman Bawankule, Rupesh Kumar Dewang, and Anil Kumar Singh. Historical data based approach to mitigate stragglers from the reduce phase of mapreduce in a heterogeneous hadoop cluster. *Clust. Comput.*, 25(5):3193–3211, 2022.
- [6] Jeffrey Dean and Sanjay Ghemawat. Mapreduce: Simplified data processing on large clusters. *Commun. ACM*, 51(1):107–113, 2008.
- [7] Aurick Qiao, Sang Keun Choe, Suhas Jayaram Subramanya, Willie Neiswanger, Qirong Ho, Hao Zhang, Gregory R. Ganger, and Eric P. Xing. Pollux: Co-adaptive cluster scheduling for goodput-optimized deep learning. In *OSDI*. USENIX Association, 2021.
- [8] Yimin Jiang, Yibo Zhu, Chang Lan, Bairen Yi, Yong Cui, and Chuanxiong Guo. A unified architecture for accelerating distributed DNN training in heterogeneous GPU/CPU clusters. In *OSDI*, pages 463–479. USENIX Association, 2020.
- [9] Yixiao Gao, Qiang Li, Lingbo Tang, Yongqing Xi, Pengcheng Zhang, Wenwen Peng, Bo Li, Yaohui Wu, Shaozong Liu, Lei Yan, Fei Feng, Yan Zhuang, Fan Liu, Pan Liu, Xingkui Liu, Zhongjie Wu, Junping Wu, Zheng Cao, Chen Tian, Jinbo Wu, Jiayi Zhu, Haiyong Wang, Dennis Cai, and Jiasheng Wu. When cloud storage meets RDMA. In *NSDI*, pages 519–533. USENIX Association, 2021.
- [10] Chuanxiong Guo, Haitao Wu, Zhong Deng, Gaurav Soni, Jianxi Ye, Jitu Padhye, and Marina Lipshteyn. RDMA over commodity ethernet at scale. In *SIGCOMM*, pages 202–215. ACM, 2016.
- [11] Radhika Mittal, Vinh The Lam, Nandita Dukkhipati, Emily R. Blem, Hassan M. G. Wassel, Monia Ghobadi, Amin Vahdat, Yaogong Wang, David Wetherall, and David Zats. TIMELY: rtt-based congestion control for the datacenter. In *SIGCOMM*, pages 537–550. ACM, 2015.
- [12] Xinhao Kong, Yibo Zhu, Huaping Zhou, Zhuo Jiang, Jianxi Ye, Chuanxiong Guo, and Danyang Zhuo. Collie: Finding performance anomalies in RDMA subsystems. In *NSDI*, pages 287–305. USENIX Association, 2022.
- [13] Yibo Zhu, Haggai Eran, Daniel Firestone, Chuanxiong Guo, Marina Lipshteyn, Yehonatan Liron, Jitendra Padhye, Shachar Raindel, Mohamad Haj Yahia, and Ming Zhang. Congestion control for large-scale RDMA deployments. In *SIGCOMM*, pages 523–536. ACM, 2015.
- [14] Gautam Kumar, Nandita Dukkhipati, Keon Jang, Hassan MG Wassel, Xian Wu, Behnam Montazeri, Yaogong Wang, Kevin Springborn, Christopher Alfeld, Michael Ryan, et al. Swift: Delay is simple and effective for congestion control in the datacenter. In *SIGCOMM*, pages 514–528, 2020.
- [15] Arjun Singhvi, Aditya Akella, Dan Gibson, Thomas F. Wenisch, Monica Wong-Chan, Sean Clark, Milo M. K. Martin, Moray McLaren, Prashant Chandra, Rob Cauble, Hassan M. G. Wassel, Behnam Montazeri, Simon L. Sabato, Joel Scherpelz, and Amin Vahdat. Irma: Re-imagining remote memory access for multi-tenant datacenters. In *SIGCOMM*, pages 708–721. Association for Computing Machinery, 2020.
- [16] Youmin Chen, Youyou Lu, and Jiwu Shu. Scalable RDMA RPC on reliable connection with efficient resource sharing. In *EuroSys*, pages 19:1–19:14. ACM, 2019.
- [17] Ran Shu, Peng Cheng, Guo Chen, Zhiyuan Guo, Lei Qu, Yongqiang Xiong, Derek Chiou, and Thomas Moscibroda. Direct universal access: Making data center resources available to FPGA. In *NSDI*, pages 127–140. USENIX Association, 2019.
- [18] Eric Shun Fukuda, Hiroaki Inoue, Takashi Takenaka, Da-hoo Kim, Tsunaki Sadahisa, Tetsuya Asai, and Masato Motomura. Caching memcached at reconfigurable network interface. In *FPL*, pages 1–6. IEEE, 2014.

- [19] Antoine Kaufmann, Simon Peter, Naveen Kr. Sharma, Thomas E. Anderson, and Arvind Krishnamurthy. High performance packet processing with flexnic. In *ASPLOS*, pages 67–81. ACM, 2016.
- [20] Saksham Agarwal, Rachit Agarwal, Behnam Montazeri, Masoud Moshref, Khaled Elmeleegy, Luigi Rizzo, Marc Asher de Kruijf, Gautam Kumar, Sylvia Ratnasamy, David E. Culler, and Amin Vahdat. Understanding host interconnect congestion. In *HotNets*, pages 198–204. ACM, 2022.
- [21] Renato Recio, Bernard Metzler, Paul Culley, Jeff Hilland, and Dave Garcia. A remote direct memory access protocol specification. Technical report, 2007.
- [22] Zhenyuan Ruan, Malte Schwarzkopf, Marcos K. Aguilera, and Adam Belay. Aifm: High-performance, application-integrated far memory. *OSDI’20*, 2020.
- [23] Youngmoon Lee, Hasan Al Maruf, Mosharaf Chowdhury, Asaf Cidon, and Kang G. Shin. Hydra : Resilient and highly available remote memory. *FAST’22*, February 2022.
- [24] Nvidia connectx-5 ndr 100g infiniband adapter card. <https://www.nvidia.com/en-us/networking/ethernet/connectx-5/>.
- [25] Nvidia connectx-7 ndr 400g infiniband adapter card. <https://nvdam.widen.net/s/srdqzxd5/connectx-7-datasheet>.
- [26] Kevin Fang and David Peng. Netdam: Network direct attached memory with programmable in-memory computing isa. *arXiv preprint arXiv:2110.14902*, 2021.
- [27] Mohammad Alian and Nam Sung Kim. Netdim: Low-latency near-memory network interface architecture. In *MICRO*, pages 699–711. ACM, 2019.
- [28] Boris Pismenny, Liran Liss, Adam Morrison, and Dan Tsafir. The benefits of general-purpose on-nic memory. In *ASPLOS*, pages 1130–1147. ACM, 2022.
- [29] Arnold O Allen. *Probability, statistics, and queueing theory*, page 259. Gulf Professional Publishing, 1990.
- [30] Ram Huggahalli, Ravi R. Iyer, and Scott Tetrick. Direct cache access for high bandwidth network I/O. In *ISCA*, pages 50–59. IEEE Computer Society, 2005.
- [31] Intel® data direct i/o technology (intel® ddio): A primer. <https://www.intel.com/content/www/us/en/io/data-direct-i-o-technology.html> Accessed Nov 30, 2022.
- [32] Arm cache stashing. <https://developer.arm.com/documentation/102407/0100/Cache-stashing> Accessed Nov 30, 2022.
- [33] Marina Vemmou, Albert Cho, and Alexandros Daglis. Patching up network data leaks with sweeper. In *MICRO*, pages 464–479. IEEE, 2022.
- [34] Alireza Farshin, Amir Roozbeh, Gerald Q. Maguire Jr., and Dejan Kostic. Reexamining direct cache access to optimize I/O intensive applications for multi-hundred-gigabit networks. In *ATC*, pages 673–689. USENIX Association, 2020.
- [35] Amin Tootoonchian, Aurojit Panda, Chang Lan, Melvin Walls, Katerina J. Argyraki, Sylvia Ratnasamy, and Scott Shenker. Resq: Enabling slos in network function virtualization. In *NSDI*, pages 283–297. USENIX Association, 2018.
- [36] Yifan Yuan, Mohammad Alian, Yipeng Wang, Ren Wang, Iliia Kurakin, Charlie Tai, and Nam Sung Kim. Don’t forget the I/O when allocating your LLC. In *ISCA*, pages 112–125. IEEE, 2021.
- [37] Elastic compute cloud (ec2). <https://aws.amazon.com/ec2> Accessed Dec 12, 2022.
- [38] IEEE. 802.11Qbb. Priority based flow control, 2011.
- [39] Intel® resource director technology (intel® rdt), 2021. <https://www.intel.cn/content/www/cn/zh/architecture-and-technology/resource-director-technology.html> Accessed Dec 13, 2022.
- [40] Mellanox neo-host. <https://support.mellanox.com/s/productdetails/a2v5000000N201AAK/mellanox-neohost> Accessed Dec 12, 2022.
- [41] Intel® performance counter monitor. <https://www.intel.com/software/pcm> Accessed Dec 12, 2022.
- [42] Intel® xeon® processor e5. <https://ark.intel.com/content/www/us/en/ark/products/64597/intel-xeon-processor-e52665-20m-cache-2-40-ghz-8-00-gts-intel-qpi.html>.
- [43] Amd 3rd gen amd epyc™ cpus. <https://www.amd.com/en/claims/epyc3x> Accessed Nov 30, 2022.
- [44] Infiniband trade association. infinibandtm architecture specification volume 1, release 1.6, published july 15, 2022.
- [45] Anuj Kalia, Michael Kaminsky, and David G. Andersen. Design guidelines for high performance RDMA systems. In *ATC*, pages 437–450. USENIX Association, 2016.



- [46] Behnam Montazeri, Yilong Li, Mohammad Alizadeh, and John Ousterhout. Homa: A receiver-driven low-latency transport protocol using network priorities. In *SIGCOMM*, pages 221–235, 2018.
- [47] Jeff Bonwick. The slab allocator: An Object-Caching kernel. In *USENIX Summer 1994 Technical Conference*. USENIX Association, 1994.
- [48] Nvidia® mellanox® connectx®-5. <https://www.nvidia.com/en-us/networking/ethernet/connectx-5/> Accessed Dec 12, 2022.
- [49] Huiba Li, Yifan Yuan, Rui Du, Kai Ma, Lanzheng Liu, and Windsor Hsu. DADI: block-level image service for agile and elastic application deployment. In *ATC*, pages 727–740. USENIX Association, 2020.
- [50] Google protocol buffers. <https://developers.google.com/protocol-buffers/> Accessed Dec 12, 2022.
- [51] Rui Miao, Lingjun Zhu, Shu Ma, Kun Qian, Shujun Zhuang, Bo Li, Shuguang Cheng, Jiaqi Gao, Yan Zhuang, Pengcheng Zhang, Rong Liu, Chao Shi, Binzhang Fu, Jiaji Zhu, Jiasheng Wu, Dennis Cai, and Hongqiang Harry Liu. From luna to solar: the evolutions of the compute-to-storage networks in alibaba cloud. In *SIGCOMM*, pages 753–766. ACM, 2022.
- [52] Nvidia® connectx®-6 dx. <https://www.nvidia.com/en-us/networking/ethernet/connectx-6-dx/> Accessed Dec 12, 2022.
- [53] Introduction to cache allocation technology in the intel xeon processor e5 v4 family. <https://www.intel.cn/content/www/cn/zh/developer/articles/technical/introduction-to-cache-allocation-technology.html> Accessed Nov 30, 2022.
- [54] Fio. <https://github.com/axboe/fio> Accessed Nov 22, 2022.
- [55] Korakit Seemakhupt, Sihang Liu, Yasas Senevirathne, Muhammad Shahbaz, and Samira Manabi Khan. Pmnet: In-network data persistence. In *ISCA*, pages 804–817. IEEE, 2021.
- [56] David Sidler, Zeke Wang, Monica Chiosa, Amit Kulka-rni, and Gustavo Alonso. Strom: smart remote memory. In *EuroSys*, pages 29:1–29:16. ACM, 2020.
- [57] Nikita Lazarev, Shaojie Xiang, Neil Adit, Zhiru Zhang, and Christina Delimitrou. Dagger: efficient and fast rpcs in cloud microservices with near-memory reconfigurable nics. In *ASPLOS*, pages 36–51. ACM, 2021.
- [58] Daehyeok Kim, Amirsaman Memaripour, Anirudh Badam, Yibo Zhu, Hongqiang Harry Liu, Jitu Padhye, Shachar Raindel, Steven Swanson, Vyas Sekar, and Srinivasan Seshan. Hyperloop: Group-based nic-offloading to accelerate replicated transactions in multi-tenant storage systems. *SIGCOMM’18*, 2018.
- [59] Anuj Kalia, Michael Kaminsky, and David G. Andersen. Fasst: Fast, scalable and simple distributed transactions with two-sided (rdma) datagram rpcs. *OSDI’16*, 2016.
- [60] Anuj Kalia, Michael Kaminsky, and David G. Andersen. Datacenter rpcs can be general and fast. *NSDI’19*, 2019.
- [61] Siyu Yan, Xiaoliang Wang, Xiaolong Zheng, Yinben Xia, Derui Liu, and Weishan Deng. Acc: Automatic ecn tuning for high-speed datacenter networks. In *SIGCOMM*. Association for Computing Machinery, 2021.
- [62] Yuliang Li, Rui Miao, Hongqiang Harry Liu, Yan Zhuang, Fei Feng, Lingbo Tang, Zheng Cao, Ming Zhang, Frank Kelly, Mohammad Alizadeh, et al. Hpsc: High precision congestion control. In *SIGCOMM*, pages 44–58. 2019.
- [63] Kevin T. Lim, David Meisner, Ali G. Saidi, Parthasarathy Ranganathan, and Thomas F. Wenisch. Thin servers with smart pipes: designing soc accelerators for memcached. In *ISCA*, pages 36–47. ACM, 2013.